17th World Conference on Earthquake Engineering, 17WCEE
Sendai, Japan - September 13th to 18th 2020

Dynamic behavior of the Partial Floating Sheet-pile method

T. Tobita[(1)], K. Kashiwagi[(2)], N. Inoue[(3)], and J. Otani[(4)]

[(1)] *Associate Professor, Kansai University, tobita@kansai-u.ac.jp*
[(2)] *Graduate student, Kyoto University, kashiwagi.kei.z88@st.kyoto-u.ac.jp*
[(3)] *Penta Ocean, Co. Ltd.*
[(4)] *Professor, Kumamoto University, junotani@kumamoto-u.ac.jp*

Abstract

To reduce settlements and lateral deformations associated with river dykes/embankments constructed on soft soils, sheet-pile methods have often been employed as mitigation measures (Ochiai et al. 1991). Affected areas of the settlements/lateral deformations are often stretched to surrounding ground nearby.

The grounding sheet-pile method (hereafter called GSP) is a conventional method and is consisted of a series of grounding sheet-piles which are driven into the bearing layer (Koseki et al. 2009: Otsushi et al. 2011). Although this method is effective in reducing settlement due to consolidation, economic efficiency and workability are low when a soft soil layer is thick.

The floating sheet-pile method, not driven into the bearing layer, has an advantage on economic efficiency and workability over the grounding sheet-pile method. However, effectiveness in reducing ground deformation is obviously lower than the grounding sheet pile.

The Partial floating sheet-pile method (hereafter called PFS method) is a combination of the grounding sheet-piles and floating sheet-piles (Research group on the PFS method, 2005). There are a number of experimental studies related to the PFS method, e.g, Hagisako (2000), Eguchi(2002), Nakazawa et al. (2011), Kijima (2018), Muto (2018), Kashiwagi (2019), Inoue (2019).

In 2016 Kumamoto, Japan, earthquake, severe ground motion caused significant damages not only to residential houses or slopes, but also to embankments and levees due to liquefaction. It was reported that some embankments reinforced with the PFS method suffered minor damages, though its mechanism is yet unknown. Thus, the objective of this study is to investigate the behaviour of the PFS method under dynamic conditions.

A series of centrifuge experiments are conducted to investigate mitigation measures of soft soils with sheet pile method. Characteristics of two types of sheet piles, Grounding Sheet Pile and Partial Floating Sheet pile, are compared with each other and with the case of no measures. The ground was either single pseudo-over-consolidated clay or loose saturated sand over pseudo-over-consolidated clay.

Performance of the PFS under the dynamic condition taken in this particular study was comparable to that of the GSP. Profiles of the residual bending moment of these sheet piles showed similar trends on the depth of peak values. For the case of single clay layer, this might be because deformation of the ground induced by the settlement of the embankment might be limited near the ground surface. For the case of loose saturated sand/clay layer, this might be because embedded length of 1 m in the clay layer of the floating part of the PFS was deep enough to sustain the deformation of the PFS comparable to the GSP.

Performance of the PFS method may be acceptable under the moderate loading conditions considered in this study. However, its performance under various realistic conditions should be investigated in detail to validate its practical application.

Keywords: Sheet-pile method, Centrifuge modelling, Dynamic, Consolidation, Liquefaction

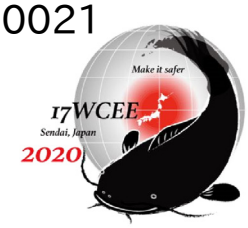

1. Introduction

Embankments constructed on soft clay ground cause not only settlements but also lateral deformations (e.g., Sekiguchi and Shibata, 1986). Affected area of the settlements/lateral deformations is often stretched to surrounding ground nearby. To reduce such a deformation, sheet-pile methods have often been employed as mitigation measures (Ochiai et al. 1991).

The grounding sheet-pile method (hereafter called GSP) (Fig. 1(a)) is a conventional method and is consisted of a series of grounding sheet-piles which are driven into the bearing layer (Koseki et al. 2009: Otsushi et al. 2011). Although this method is effective in reducing settlement due to consolidation, economic efficiency and workability are low when a soft soil layer is thick.

The floating sheet-pile method, not driven into the bearing layer, has an advantage on economic efficiency and workability over the grounding sheet-pile method. However, effectiveness in reducing ground deformation is obviously lower than the grounding sheet pile.

The Partial floating sheet-pile method (hereafter called PFS method, Fig. 1(b)) is a combination of the grounding sheet-piles and floating sheet-piles (Research group on the PFS method, 2005). There are a number of experimental studies related to the PFS method, e.g, Hagisako (2000), Eguchi(2002), Nakazawa et al. (2011), Kijima (2018), Muto (2018), Kashiwagi (2019), Inoue (2019).

In 2016 Kumamoto, Japan, earthquake, severe ground motion caused significant damages not only to residential houses or slopes, but also to embankments and levees due to liquefaction. It was reported that some embankments reinforced with the PFS method suffered minor damages, though its mechanism is yet unknown. Thus, the objective of this study is to investigate the behaviour of the PFS method under dynamic conditions.

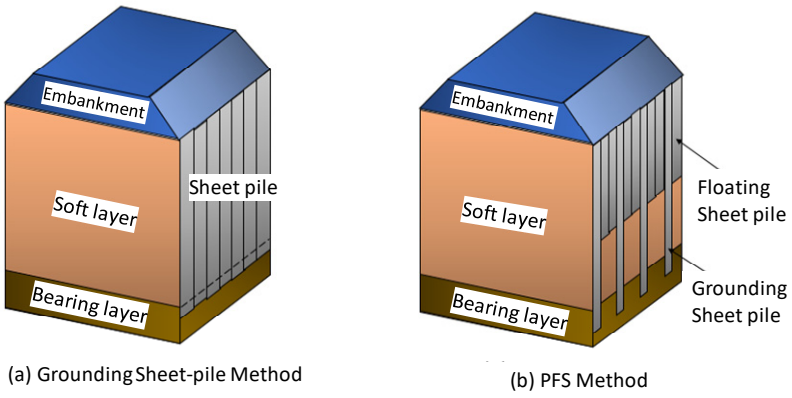

Fig. 1. Overview of sheet-pile countermeasures: (a) The Grounding sheet-pile method (GSP), and (b) PFS method

2. Overview of experiments

2.1. Centrifuge apparatus

The beam type centrifuge apparatus whose radius is 1.5 m in Kansai university was used. This apparatus with a shaking table driven by the hydraulic actuator can shake a model during flight. All experiments were carried out under 50 G (G denotes acceleration due to gravity = 9.8 m/s^2) with 1/50 scale. The conventional scaling law of centrifuge modelling is shown in Table 1 (e.g., Garnier et al. (2007)). In what follows, the values are in prototype scale unless otherwise noted.

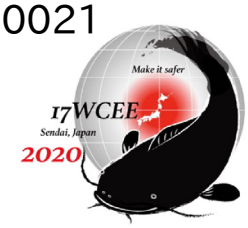

Table 1 Scaling law in N G centrifugal field (e.g., Garnier et al. (2007)).

Items	Scaling factors (prototype/model)
Length	*N*
Velocity	*1*
Acceleration	*1/N*
Time	*N*
Density	*1*
Stress	*1*
Strain	*1*
Deformation	*N*
Viscosity	*N*

2.2. Preparation of the model ground

Model ground is constructed in a rigid container (450L x 200D x 395H mm in model scale). It is composed of either a single clay layer (10 m thick) (Fig. 2(a)) or sand layer (5 m thick) on top of a clay layer (5 m thick) (hereafter called "sand/clay layer") (Fig. 2(b)). Dimension of the model ground is 22.5 m in length, 10 m in height, and 10 m in depth.

Clay layers in this experiment was prepared as a pseudo-over-consolidated clay by mixing Kaolin with gypsum and water to reduce the time required for model ground consolidation (Kijima et al., 2018). In this study, it is called Kaolin/Gypsum clay. To make the clay, firstly, two types of materials are prepared, i.e., the material A and B. Material A is composed of water and gypsum whose mass ratio is water/gypsum = 2/5. Material B is composed of water and Kaolin with water/Kaolin = 4/5. The unconfined compression strength of the clay can be controlled by changing the mixture ratio of material A and B. Fig. 3 represents the relationship between the mass percentage of material A in Kaolin/Gypsum soil and the unconfined compression strength, q_u, and the deformation modulus, E_{50}. The unconfined compression strength increases linearly as the percentage of the material A increases. In contrast, the values of modulus of deformation, E_{50}, suddenly increases from 2,000 kPa to 4,700 kPa at 10% of Material A. In this study, mass ratio between material A/B = 1/9 was chosen to have the unconfined compression strength in a range of 20 to 30 kPa.

From the *e*-log*p* curve (Fig. 4), the pre-consolidation stress of the Kaolin/Gypsum clay with the above mass ratio is determined to be 113 kPa and compressive index, C_C and swelling index, C_S are, respectively, 0.685 and 0.039 (Table 2). The plasticity chart in Fig. 5 indicates that the Kaolin/Gypsum clay is categorized as "MH" or "CH."

To construct the saturated loose sand layer of the relative density of Dr=50% with Toyoura sand (Table 3), the water pluviation with the methylcellulose solution whose viscosity was adjusted to 50 cSt at 20 °C was employed.

Five accelerometers were placed as shown in Fig. 2 (Input, and Acc1 to Acc4). 4 pore water pressure transducers were placed as in Fig. 2 (P1 to P4). The strains along the center axis of the model sheet-pile on both sides were measured at 5 sections (SG1 to SG10 in Fig. 2). In addition, settlements of ground surface were measured by hand at the designated 21 locations on the ground surface (see Fig. 7). Also, lateral displacement at the top edge of the model sheet-pile was measured by hand.

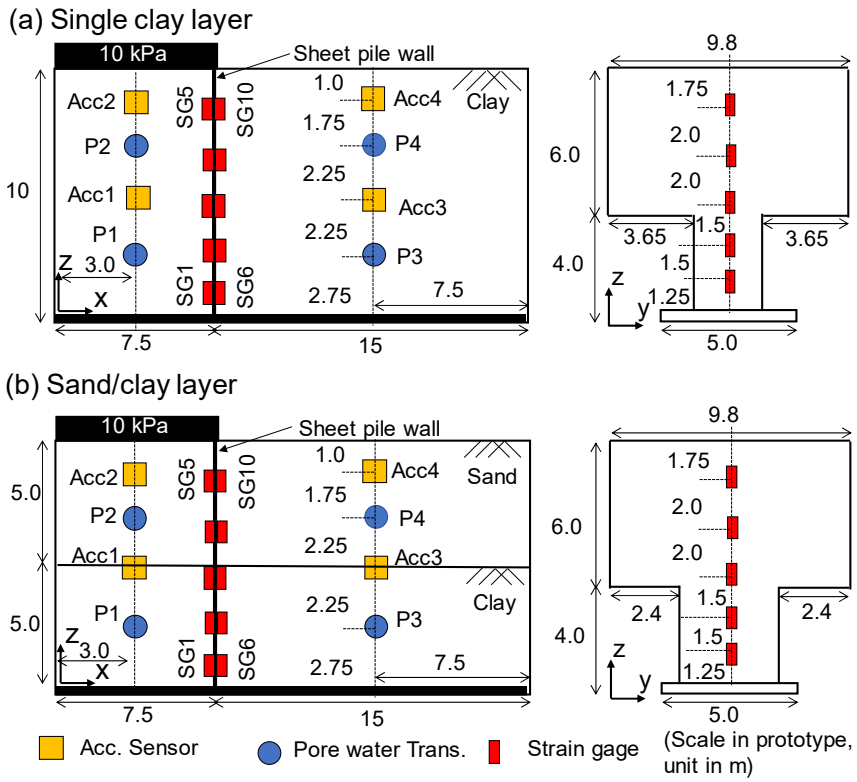

Fig. 2. Cross sections of model sheet-piles, ground conditions, and sensor locations: (a) Case 1 to 3 with single clay layer (b) Case 4 to 6 with sand/clay layer.

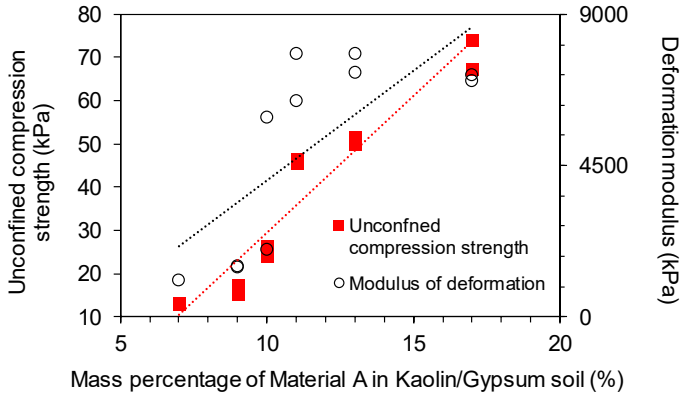

Fig. 3. Unconfined compression strength, q_u, and deformation modulus, E_{50}, versus mass ratio of material A of Kaolin/Gypsum clay.

2.3. Sheet-pile models and test cases

Model sheet-piles are made of stainless plate (Table 4). They are placed at 7.5 m from the left side wall of the container and were welded to the bottom plate for a rigid boundary condition. As shown in Fig. 2, for GSP, the shape of the plate is rectangular, while for PFS, the bottom part of the rectangular plate is cut to

form a T-shape. It is assumed that for the PFS, the T-shape constitutes one unit of the sheet-piles and it is virtually infinitely placed side by side.

Six test cases were employed as listed in Table 5. For Cases 4 to 6, due to technical reasons (malfunctioning of strain gages), as shown in Fig. 2(b), different model sheet pile whose width of the floating part was different from Case 1 to 3 was used. Width of grounding part is 3.65 m for Case 1 to 3 (Fig. 2(a) and Fig. 6), while that is 2.4 m for Case 4 to 6 (Fig. 2(b)). Both sheet-pile models mentioned above have the same height of floating part and their bottom is driven into the clay layer about 1 m (see Fig. 2(b) for Case 3 and 6).

Instead of using soil as an embankment, a steel plate was placed on the ground surface (Fig. 7) to keep constant overburden load of 10 kPa.

Table 2. Properties of Kaolin/Gypsum clay.

Clay	Kaolin/Gypsum
Soil Classification	MH
Cc	0.685
Cs	0.039
p_c (kPa)	113
q_u (kPa)	20 - 30
E_{50} (kPa)	2,000 - 5,000

Table 3. Properties of sandy ground for Case 4 to 6.

Sand	Toyoura
G_s	2.661
e_{max}	0.983
e_{min}	0.609
Viscosity (cSt)	50

Table 4. Properties of the model sheet pile (Amma and Tsukuni, 2007).

Target sheet pile	Type FSP-3
Young's modulus (GPa)	210
Flexural rigidity EI (MNm^2)	35.28

Table 5. Test cases.

Case	Sheet-pile type	Ground
1	NOC (NO Countermeasure)	Single Clay
2	GSP (Grounding Sheet-Pile)	
3	PFS (Partial Floating Sheet-pile)	
4	NOC	Sand/Clay
5	GSP	
6	PFS	

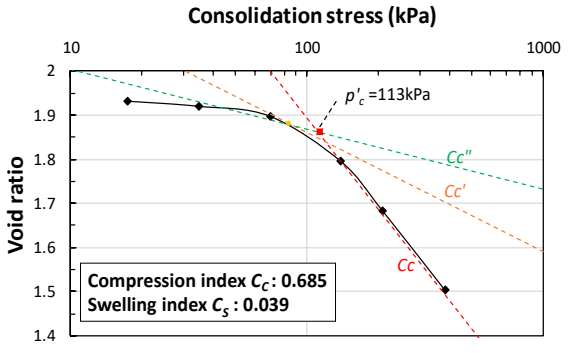

Fig. 4. *e*-log*p* curve of the Kaolin/Gypsum clay.

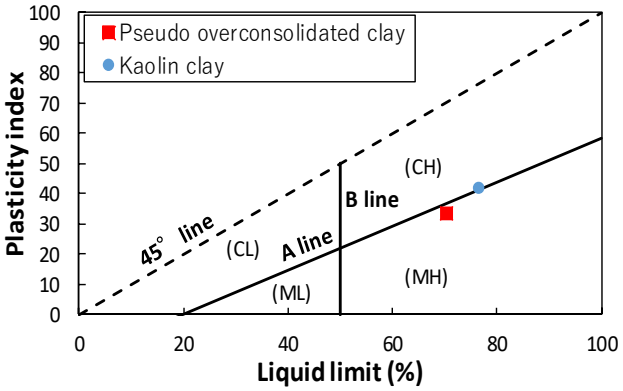

Fig. 5. Plasticity chart of Kaolin/Gypsum clay of material A/B=1/9

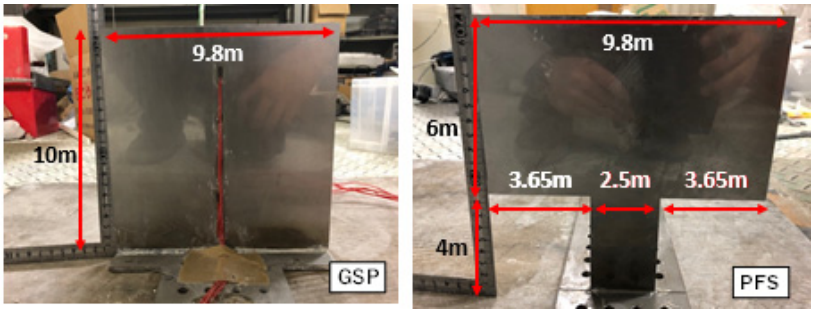

Fig. 6. Model sheet-piles for Case 1 to 3: (Left: GSP, Right: PFS).

Fig. 7. Top view of single clay layer before the initial flight. Left grey part is the steel plate to give equivalent load to an embankment.

2.4. Test procedures

There are some differences in test procedures between the cases of single clay layer (Case 1 to 3) and those of sand/clay layer (Case 4 to 6).

For the cases of single clay layer (Case 1 to 3), after constructing the model ground in 1 G, the model was kept under 50 G for one hour (in model scale) for consolidation. Next, the surface settlements were measured by hand in 1 G as mentioned earlier. Then, a tapered sin wave whose duration is 36 s is given as an input motion (Fig. 8).

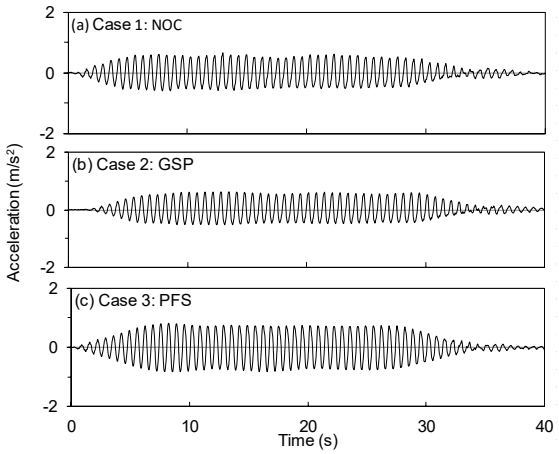

Fig. 8. Measured input acceleration: (a) Case 1, (b) Case 2, and (c) Case 3.

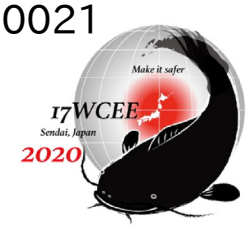

Target peak amplitude of the input acceleration and the dominant frequency are respectively about 0.5m/s^2 and 1.5Hz. As shown in Fig. 8(c), the peak amplitude for Case 3 (PFS)was by accident slightly larger than the others. After shaking, the model was kept under 50 G for one hour (in model scale) for reconsolidation.

For the cases of sand/clay layer (Case 4 to 6), the model was spun under 50 G for 5 minutes (in model scale) to stabilize the sand layer. After measuring the ground height in 1 G, the model was again spun up to 50 G. Then, shaking was given to the model. The maximum amplitude and the dominant frequency, differ from those of single clay layer (Case 1 to 3), are, respectively, 1.5 m/s^2 and 1.0 Hz. This is because liquefaction could not be reproduced with the input motion used in Case 1 to 3. The model was kept under 50 G until the excess pore water pressure in the sand layer was completely dissipated.

In all cases, the level of ground surface and displacement of the top of the sheet-pile was measured by hand.

3. Test results

3.1. Cases of single clay layer (Case 1 to 3)

Time histories of response acceleration show amplification in the clay layer (Fig. 9). The amplification is slightly larger in the free field motion (Fig. 9(c) and (d)) than those underneath the embankment (Fig. 9(a) and (b)). This may be because elastic/plastic modulus in the ground underneath the embankment was larger due to the surcharge. A major reason for the larger amplitude in the case of PFS (Fig. 9(b) and (d) in Case 3) is simply due to larger input motion accidentally given to the model.

Fig. 10 shows time histories of excess pore water pressure ratio (hereafter abbreviated as EPR) with the initial excess pore water pressure being set to 0 by assuming that the excess pore water pressure due to consolidation is completely dissipated before shaking. In Fig. 10, some data indicated in the figures are missing due to malfunctioning of pore water pressure transducers. It is apparent that the peaks of EPR is larger in the free field than in the ground underneath the embankment. Also, from Fig. 10(c) and (d), the peaks of the excess pore pressure in the case with sheet-piles (Case 2 and 3) tend to be much lower than that of no counter measure (Case 1)

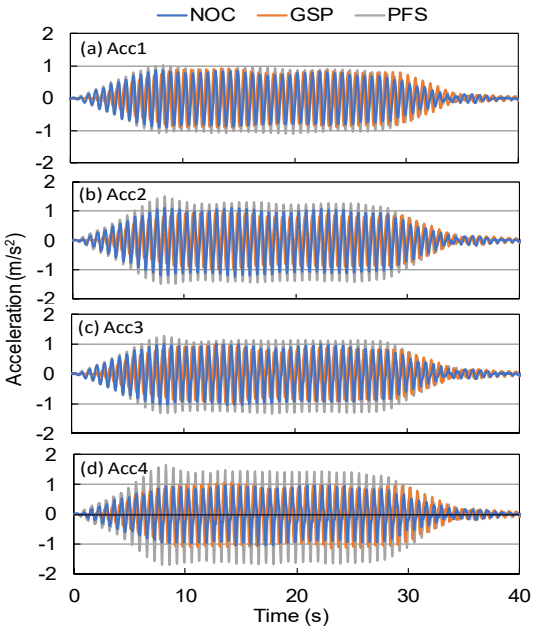

Fig. 9. Time histories of response acc. in the cases of single clay layer (Case 1 to 3): (a) Acc1, (b) Acc2, (c) Acc3, and (d) Acc4.

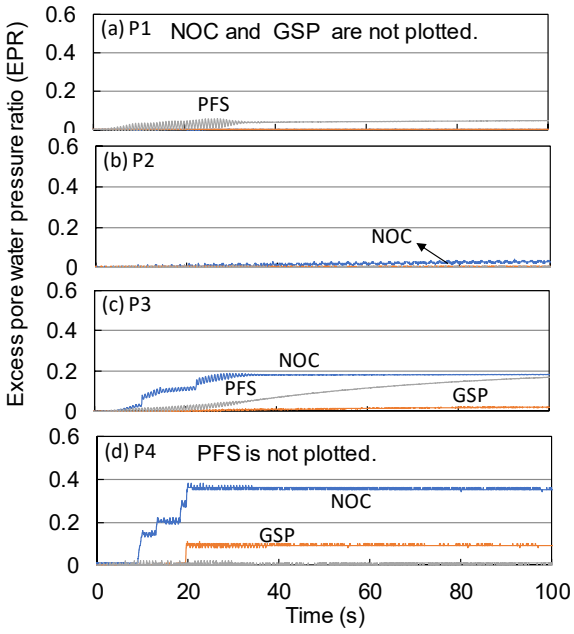

Fig. 10. Time histories of EPR in the cases of single clay layer: (a) P1, (b) P2, (c) P3, and (d) P4.

Fig. 11 shows profiles of the residual bending moment of the sheet-pile after shaking. In Case 2 (GSP) (Fig. 11(a)), the maximum moment is obtained at the depth of -1.75 m, while that of Case 3 (PFS) is -5.75 m where the shape of the sheet pile changes. Cause of large bending moment in Case 2 is due perhaps to malfunctioning of strain gauges near the surface, because the strain near the surface might be close to zero due to the rotation-free boundary condition at the pile head.

Measured surface settlement due to consolidation under 50 G (before shaking) along the x-axis (longitudinal direction of the container) in Fig. 12 show that the largest settlement in the free field occurred in the case of no countermeasure (Case 1), about 0.2 m on average. Here, the values of settlements in the longitudinal direction are the average of 3 locations in the transverse direction. The case of PFS (Case 3)

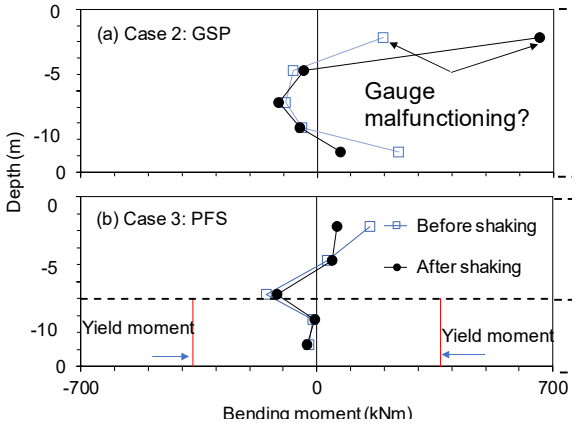

Fig. 11. Residual bending moment profile in the case of single clay layer (a) Case 2 (GSP), (b) Case 3 (PFS)

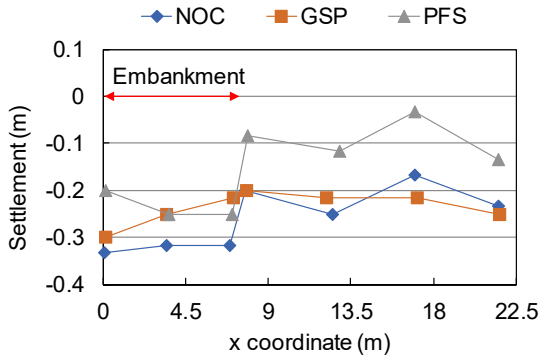

Fig. 12. Ground surface settlements before shaking in the cases of single clay layer (Case 1 to 3).

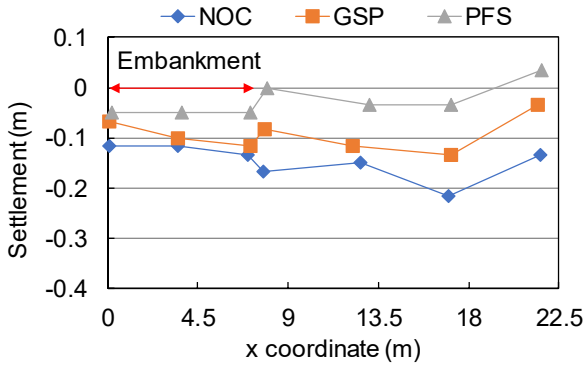

Fig. 13. Ground surface settlements after shaking (Case 1 to 3). Settlements are taken from the difference/increments from the ones before shaking.

showed the smallest settlement, about 0.1 m on average. For some reasons, the case of GSP (Case 2) shows almost the same amount of settlement with Case 1. Variability in strength parameters in the Kaolin/Gypsum clay may be the one of the causes of this observation. As shown in Fig. 12, for the settlement of the embankment, if there are no counter measures, the amount of the settlement is over 0.3 m, while with the

sheet-piles, it is on average reduced within a range of 0.2 to 0.3 m. In this study, the sheet-piles are properly working to reduce the amount of settlements.

Residual surface settlement along the x-axis after shaking is plotted in Fig. 13. Here, the amount of settlement is the increments from those before shaking (Fig. 12) and possibly due to dissipation of excess pore water pressure. From Fig. 13, settlements of free field in the case of no countermeasure (Case 1) are larger than that of the area of embankment and are much larger than the other cases. This may be due to reconsolidation associated with dissipation of the excess pore water pressure induced by shaking (Fig. 10(c) and (d)). As mentioned in Fig. 9, Fig. 10 also shows the smallest settlement in PFS (Case 3).

The average lateral displacements at the top of the sheet-pile in Case 2 (GSP) was 0.07 m after shaking, while those in Case 3 (PFS) was 0.09 m. Considering smaller value of the overall flexural rigidity in the PFS, the results are quite reasonable. However, considering the trend in the settlement (Fig. 12), this is contradictory.

3.2. Cases of sand/clay layer (Case 4 to 6)

From time histories of response acceleration in the cases of sand/clay layer (Case 4 to 6) shown in Fig. 14, the wave forms of Acc1 and Acc3 located in the clay layer is almost identical to the input motion (not shown due to page limitation), except for the case of GSP (Case 5) in Fig. 14(c) in which accelerometer was malfunctioning.

Contrary, the amplitude of the acceleration in sand layer in free field (Fig. 14(d)) is attenuated due to liquefaction. The larger amplitude appearing in the case of NOC (no countermeasure) (Case 4) in Fig. 14(d) may be associated with the cyclic mobility caused by large shear strains in the sand layer induced by large deformation of the ground due to the lack of confinement by the sheet-piles.

The amplitude of acceleration underneath the embankment (Fig. 14 (b)) show minor attenuation

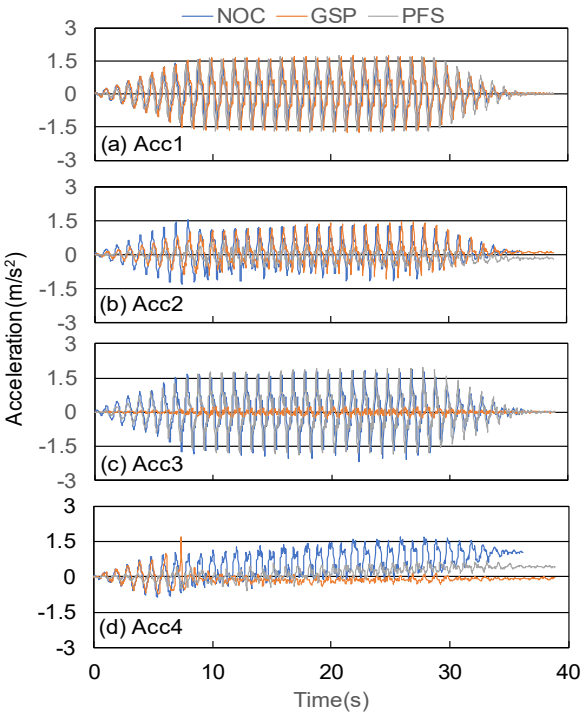

Fig. 14. Time histories of response acc. in the cases of sand/clay layer (Case 4 to 6): (a) Acc1, (b) Acc2, (c) Acc3, and (d) Acc4

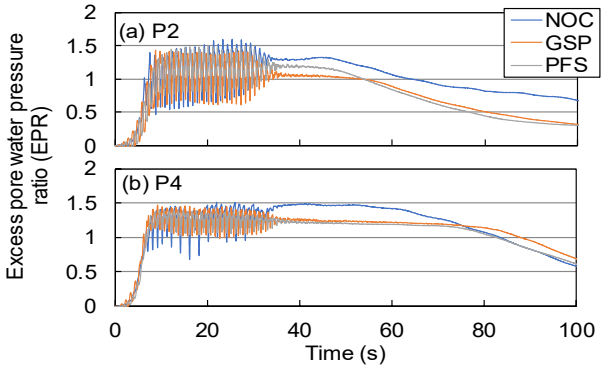

Fig. 15. Time histories of EPR on the sand/clay layer: (a) P1 and (b) P4.

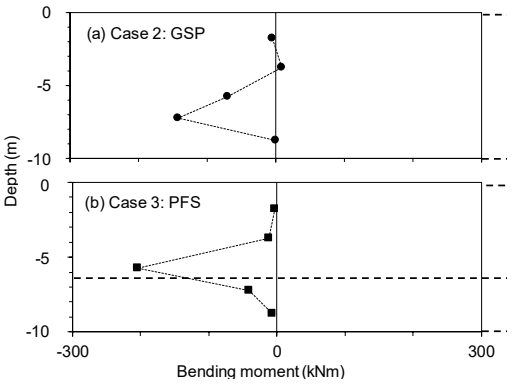

Fig. 16. Distribution of bending moment in sand/clay layer: (a) Case 5: GSP, and (b) Case 6: PFS.

compared to the ones in free field. This is due to the larger initial effective confining stress induced by the surcharge of embankment load.

Time histories of EPR in the sand layer (P2 and P4) (Fig.15) show that the all EPRs are over 1.0 indicating the occurrence of liquefaction.

Profile of residual bending moment in depth shown in Fig. 16 indicates that deformation of the model sheet pile is in elastic range after shaking. By examining the entire record of the bending moment at the gauge locations, they were all in the range below the yielding moment. In the PFS case, the largest bending moment is obtained at the gauge just above the point where the shape of the sheet pile changes. This is somewhat similar to Case 3 of single clay layer (Fig. 11(b)).

Fig. 17 shows ground surface settlements after shaking, i.e., after complete dissipation of the excess pore water pressure. In all cases, the ground surface is uplifted at the both edges of the rigid box. This is due to the radial centrifugal acceleration. Realizing this inherent adverse effect in centrifuge experiment, let us consider the settlements with Fig. 17. Settlements tend to be smaller in the model sheet-pile (Case 5 and 6) than the case of no counter measure (Case 4). The level of settlements in Case 5 and 6 is almost identical possibly indicating that both sheet-pile moved in a similar fashion.

The average residual lateral displacements of the top of the sheet pile models had slight difference 0.06m and 0.10m in the GSP and PFS, respectively. This result is consistent with the trend of settlements.

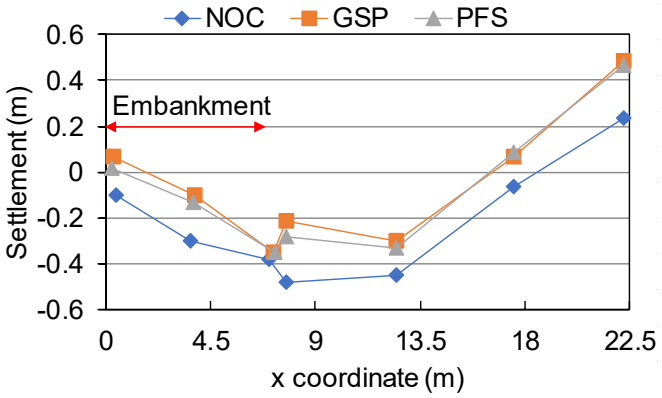

Fig. 17. Ground surface settlements after shaking (Case 4 to 6). Settlements are taken from the difference/increments from the ones before shaking.

Time histories of strains exerted on the sheet piles (Fig. 18) show that residual strain in PFS (Case 6) is the largest at SG3/SG8 where the shape of the sheet pile changes, while the largest residual strain is obtained at SG2/SG7 in GSP (Case 5). Strain amplitudes at narrow part in PFS is much smaller than those of GSP indicating the part where the cross section changes, near SG3 and SG8, is absorbing most of the deformation caused by the movement of embankment.

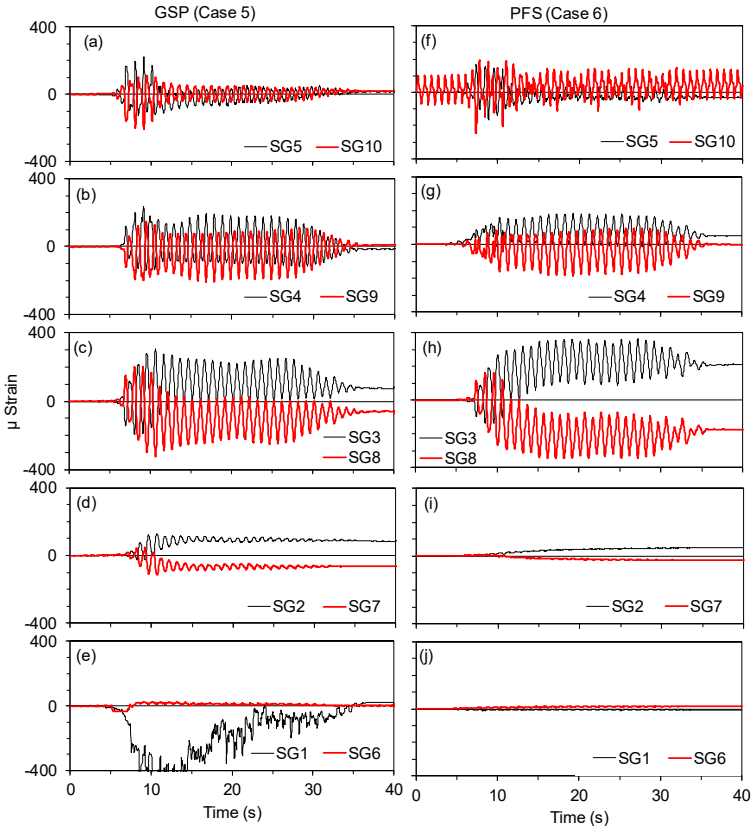

Fig. 18. Time histories of strains exerted on the model sheet piles: (a) to (e) for Case 5: GSP, and (f) to (i) for Case 6: PFS.

4. Conclusions

A series of centrifuge experiments are conducted to investigate mitigation measures of soft soils with sheet pile method. Characteristics of two types of sheet piles, Grounding Sheet Pile (GSP) and Partial Floating Sheet pile (PFS), are compared with each other and with the case of no measures (NOC). The ground was either single pseudo-over-consolidated clay or loose saturated sand over pseudo-over-consolidated clay.

Performance of the PFS under the dynamic condition taken in this particular study was comparable to that of the GSP. Profiles of the residual bending moment of these sheet piles showed similar trends on the depth of peak values. For the case of single clay layer, this might be because deformation of the ground induced by the settlement of the embankment might be limited near the ground surface. For the case of loose saturated sand/clay layer, this might be because embedded length of 1 m in the clay layer of the floating part of the PFS was deep enough to sustain the deformation of the PFS comparable to the GSP.

Performance of the PFS method may be acceptable under the moderate loading conditions considered in this study. However, its performance under various realistic conditions should be investigated in detail to validate its practical application.

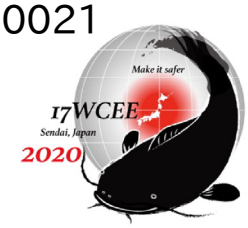

5. Acknowledgements

We would like to thank the International Press-in Association and GIKEN Ltd. for providing funds to the first author. The work was partially supported by JSPS KAKENHI Grant Number 17H008460 and 17H012872.

6. References

[1] Amma K and Tsukuni S (2007): Earthquake resisting performance of sealing sheet pile considering structural anisotropy. Doboku Gakkai Ronbunshu A, **63**(2), 326-335.

[2] Eguchi M (2002): Development of new sheet-pile mitigation measures for soft ground. Master thesis submitted to Kumamoto University, Japan.

[3] Fujiwara K, Koseki J, Otsushi K and Nakayama H. (2013): Study on reinforcement method of levees using steel sheet-piles. Foundation and soft ground Engineering Conference, Thu Dau Mot University, ICTDMU-1, Binh Duong, 281-289.

[4] Garnier J, Gaudin C, Springman SM, Culligan PJ, Goodings D, Konig D, Kutter B, Phillips R, Randolph MF and Thorel L. (2007): Catalogue of scaling laws and similitude questions in geotechnical centrifuge modelling. International Journal of Physical Modelling in Geotechnics, **7**(3), 1-23.

[5] Hagisako M. (2000): Development of new sheet-pile countermeasure method for soft ground. Mater thesis submitted to Kumamoto University, Japan.

[6] Inoue N (2019): Study on dynamic behavior of the PFS method in sand/clay ground. Graduation thesis submitted to Kansai University, Japan.

[7] Kashiwagi K (2019): Dynamic behavior of the Partial Floating Sheet-pile in clay layer. Master thesis submitted to Kansai University, Japan.

[8] Kijima N (2018): Centrifuge study about levees with the Partial floating sheet-pile method and its PIV analysis. Graduation thesis submitted to Tokushima university.

[9] Kijima N, Hizen D, Manabe S and Ueno K (2018): Characteristics of man-made clay for geotechnical centrifuge modelling. The ,53rd Japanese Geotechnical Society Annual Conference, 1041-1042.

[10] Koseki J, Tanaka H, Otsushi K, Nagao N and Kaneko M (2009): Model tests on levees reinforced with sheet piles. SEISAN-KENKYU, Institute of Industrial Science, University of Tokyo, **61**(6), 1065-1068.

[11] Muto S (2018): Centrifuge study on mitigation measures against soft soil settlements and liquefaction with the PFS method, Graduation thesis submitted to Kansai University, Japan.

[12] Nakazawa H, Sugano T and Yoshida M (2011): Shaking table tests on countermeasure against liquefaction and tsunami for coastal levee using steel sheet pile. Journal of Structural Engineering, 57A, 367-377.

[13] Ochiai H, Hayashi S, Umezaki T and Otani J (1991): Model test on sheet-pile countermeasures for clay foundation under embankment. Developments in Geotechnical Aspects of Embankments, Excavation and Buried Structures, Balasubramaniam et al. (eds), Balkema, Rotterdam, ISBN 90 5410 0192, 277-287.

[14] Ohki M, Seki M, Nagao T and Nakano M (2013): Experimental validation of five failure modes and the proposal of seismic reinforcement in the railway embankment. Journal of Japan Society of Civil Engineers, Ser. C (Geosphere Engineering), **69**(2), 174-185.

[15] Otushi K, Koseki J, Kaneko M, Tanaka H, and Nagao N (2011): Experimental study on reinforcement method of levees by sheet-pile. Japanese Geotechnical Journal, **6**(1), 1-14.

[16] Research group on the PFS method (2005): Partial Floating Sheet-Pile Method. Technical document, 2005.

[17] Sekiguchi H and Shibata T (1986): Lateral deformation of soft foundations below embankments. Annuals of Disaster Prevention Research Institute, Kyoto University, No. 29B-2, 69-81.

